Treatment of Dairy Wastewater by Electrocoagulation using Iron Filings Electrodes

*Ali W. Ahmed **1* 🆔✉, *Mohamed A. Atiya **2* 🆔✉ *and Mohanad J. M-Ridha **1* 🆔✉

[1]Department of Environmental Engineering, University of Baghdad, Baghdad, Iraq.
[2]Department of Biochemical Engineering, University of Baghdad, Baghdad, Iraq.
*Corresponding Author.

Abstract

This study investigated the treatment of dairy wastewater using the electrocoagulation method with iron filings as electrodes. The study dealt with real samples collected from local factory for dairy products in Baghdad. The Response Surface Methodology (RSM) was used to optimize five experimental variables at six levels for each variable, for estimating chemical oxygen demand (COD) removal efficiency. These variables were the distance between electrodes, detention time, dosage of NaCl as electrolyte, initial COD concentration, and current density. RSM was investigated the direct and complex interaction effects between parameters to estimate the optimum values. The respective optimum value was 1 cm for the distance between electrodes, (60 – 120) min for detention time, 250 mg NaCl/L added, $C_0/6 = 5,775$ mg COD/L as initial COD concentration, and 7.884 - 8.077 mA/cm2 as current provided. At the optimum parameter values, the optimum COD removal efficiency was 73.4%. Meanwhile, the study also performed removal efficiency for nitrogen (N) and phosphate (P) due to their effects on the aquatic life and systems. The optimum removal efficiency for phosphorus and nitrogen was 98.0% and 80.3%, respectively. Due to its effects on the environment and to comply with local legislations, treating these wastewaters using eco-friendly processes was highly recommended taking in consideration the economic feasibility, flexibility and easiness to operate. In addition, the study proved that the high surface area for iron filings played a crucial role in removing process.

Keywords: Chemical oxygen demand, Diary wastewaters, Electrocoagulation, Removal efficiency, Response Surface Methodology.

Introduction

Dairy wastewater contains many pollutants. The highest concentrations are for chemical oxygen demand (COD) and biochemical oxygen demand (BOD). Other pollutants include nitrogen (N), phosphorous (P), total dissolved solids (TDS), total solids (TS), total suspended solids (TSS), oil, and grease are found also, these parameters played an important role in estimated surface water quality[1]. In particular, N and P have attracted much attention in dairy wastewater treatment due to their eutrophication effects. While, organic matters play a crucial role in oxygen depletion within water bodies[2]. Over the past two decades, dairy industries developed rapidly in response to the ever-increasing growth of the world population[3]. The calculations of World Bank Group showed that meat and dairies products consume approximately 25% of the total freshwater that used by food and beverage industry[4]. This amount is used for cleaning, sanitizing, heating, cooling, and floor washing.

Many techniques for treating dairy wastewaters encompass using aerobic and anaerobic methods; activated sludge process, aerated lagoons, trickling filters, sequencing batch reactor, anaerobic sludge blanket (UASB), anaerobic filters, etc[5]. However, these methods are costly, consuming a high amount of energy while producing a large quantity of sludge. Various physicochemical methods are modified to treat dairy wastewater. Coagulation or flocculation is the most commonly used one[5]. In general, dairy wastewater was pre-treated using various inorganic or organic coagulants, followed by filtration, e.g., nanofiltration (NF) or reverse osmosis (RO)[6, 7].

The electrocoagulation (EC) process is considered the most promising technology for dealing with various pollutants existed in different types of wastewaters[8, 9]. This process proved it is environmentally compatible[10, 11], easy to operate, and requiring simple equipment with low retention time. In addition, no chemicals needed, while producing a relatively low quantity of sludge with rapid sedimentation[9]. Overall, EC follows three successive stages: (i) coagulant formation, (ii) contaminant (particle) destabilization, and (iii) aggregation of the coagulant as a floc[12]. Since metal waste scraps are generated massively worldwide, they are a good source for EC electrodes. Reusing these wastes is beneficial to the environment while reducing the total EC costs. However, studies on iron or aluminum wastes for EC anodes are scarce[13, 14].

Meanwhile, in experimental optimization, one factor is generally varied at a time while others are fixed as constants. However, optimization cannot recognize complex relations among factors and their responses simultaneously[14], time spent due to the large number of runs involved, along with increased use of chemical compounds. Hence, it is costly[15]. This study investigated the removal efficiency of iron-filling electrodes for treating dairy wastewaters, particularly the removal efficiency of COD, P, and N pollutants. In addition, it evaluated the complex interactions among operating parameters and the optimal conditions for the removal efficiency using Response Surface Methodology (RSM). Altogether, this study investigated five parameters: distance between electrodes (A), detention time (B), NaCl dosage (C), initial concentration of COD (D), and current density (E).

Materials and Methods

Feed

Wastewater was sampled from a holding tank of a dairy factory in Camp Sara, Al-Rusafa, Baghdad, Iraq. Samples were collected weekly for the first six months using one-liter dark bottles, and then collected as and when needed. At the factory, the wastewater was treated using the sedimentation method only before being discharged into the public waterway. Before laboratory analysis, some parameters are measured at the site such as Temperature, pH and D.O. Others are measured at laboratory such as TDS. Then, the wastewater samples were stored in dark glass bottles at 4 ^{0}C to stop all relevant biological reactions that might affect the results. The experiment began by evaluating the fluctuations of COD, P and N in the wastewater resulting from milk production. The COD values of these samples varied from 32,019 to 37,998 mg/L. This study used the most frequent reading, i.e., 34,650 mg COD/L, and it was close to the average value of 35,008 mg COD/L. The concentration of P ranged from 0.9 - 0.5 mg/L and the most frequent value, i.e., 0.5 mg/L, was used for further analysis. Meanwhile, the concentration of N varied from 1.3 - 0.4 mg/L and the most frequent value, i.e., 0.4 mg/L. Table 1, shows the main primary characteristics of dairy wastewater for the factory.

Design of Reactor

The batch experiments were conducted in a rectangular glass reactor (30 cm * 15 cm * 10 cm), the reactor has a valve that controlled the input of raw material and a valve controlled the output of the treated wastewater, respectively. The hollow electrodes (width = 13 cm, height = 9 cm, and thickness = 1.6 cm) were made from isolation material for electricity. The electrodes, opened from the top, comprised 68 circles and 5 mm in diameter, distributed uniformly over the surface area of the electrode (width * height). There were two big circles at the top corner to fix the electrodes inside the reactor. The electrodes were fed with iron

fillings, 20 g each, as raw material for forming coagulant ions, yielding a 4 cm height within the electrode. The filing length must be longer than the circle diameter of the electrodes to prevent losses. The current of each electrode was powered by three electrodes (width = 13 cm, height = 9 cm, and thickness = 1.6 cm) were made from isolation material for electricity. The electrodes, opened from the top, comprised 68 circles and 5 mm in diameter, distributed uniformly over the surface area of the electrode (width * height). There were two big circles at the top corner to fix the electrodes inside the reactor. The electrodes were fed with iron fillings, 20 g each, as raw material for forming coagulant ions, yielding a 4 cm height within the electrode. The filing length must be longer than the circle diameter of the electrodes to prevent losses. The current of each electrode was powered by three rods made from the same iron fillings material. These rods were distributed uniformly over the electrodes and connected by suitable cables with a regulated power supply (model: Yaogong YG 1502 DD, 0 - 2 A, and 0 - 15 V). The reactor was set on the stirrer (model: Wine Swirl ESD001). The iron fillings and each rod were weighed using a digital tabletop scale (Kern, ABS 120-4, No. WB1200239, Germany). COD values were measured using a photometer (model: Lovibond 2420722 Vario HR-COD VARIO tube test 0 – 15,000 mg/L). The concentrations of P and N were measured using ion chromatography (Cecil, 2013, UK). The electrodes were connected in a Monopolar-Parallel configuration. Fig. 1 shows the schematic of the reactor design, while Fig. 2. shows the experimental setup.

Experimental Work

The experiment began with four electrodes. The reactor was placed on a stirrer, agitating at 100 rpm to homogenize the wastewater–flocs mixture[16]. All experiments were conducted at room temperature. The main parameters optimized are as in Table 2. Due to using scrap iron as a source for Fe ions, the surface area will be very high; the surface area of iron filings was approximately 5000 cm^2. Increasing conductivity will elevate the current at constant voltage. This will ensure that current will flow and cover all the scrap material. On the other hand, batch experiments had a great importance in estimating the limits for the design experiments

program and to understand the single behavior of each parameter. The efficiency of the experiments was calculated basing on the removal percentage. The removal efficiency percentage was calculated by (Eq. 1) below[17]:

COD Removal efficiency = $(C_0-C)/C_0$ 100 ……. 1

Where C_0 is the initial (COD, P or N) concentration (mg/L) and C is the final (COD, P or N) concentration (mg/L) at the end of the experiment. Each experiment used 2 L of wastewaters. At the end of each experiment, the iron filings and rods were washed by 0.1 N HCl, 0.1 N NaOH, and then distilled water[17] and left one day at room temperature to dry. The iron filings and rods were then weighed again to calculate the amount of dissociated iron.

Experimental Setup by Design Program

The RSM design method was used to optimize the five parameters based on the factorial technique to calculate their complex interaction for reducing the number of experiments[14, 18]. The optimization encompassed three stages: (i) RSM designing, (ii) computing the model coefficients, and (iii) validating the applied model[14]. The removal efficiency of EC based on the second-order quadratic model was computed using (Eq. 2)[19, 20] below:

$$Y= \beta_0 + \sum\beta_iX_i + \sum\sum\beta_{ij}X_iX_j + \beta_{ii}(X_{jj})^2 + \mathcal{E} ……. 2$$

Where Y is the response value, β_0 is the intercept point, while β_i, β_{ij}, and β_{ii} are the coefficients of the first, second-order polynomial equation, and binary interactions, respectively, x_i is the independent factor, and $\mathcal{E}$ is the model error.

The optima RSM design implemented in the design expert (version 10.0.3, Stat-Ease, USA) was used to evaluate the removal efficiency for the COD and the coefficients of the second-order polynomial model based on parameters and 31 experiments. The removal efficiency for COD was assumed as a response of the system (y-axis). Table 3 shows the parameters, ranges, and coded values. Table 4 lists all the experiments constructed by the program. The coefficient of determination (R^2) was calculated using Eq. 3 below[14]:

$$R^2 = 1-\{[\sum r_{i,exp} – r_{i,cal})]/\sum[r_{i,exp}-(r_{i,exp}/n)^2]\} …….. 3$$

Meanwhile, the adjusted coefficient of determination $(R_{adj})^2$ was calculated using Eq. 4 below:

$$R_{adj}^2 = \{1-[\sum(r_{i,exp}-r_{i,cal})^2/\sum(r_{i,exp}-\acute{r}_{i,exp})^2]\}*[(n-1)/(n-p-1)]\dots\dots 4$$

The relationship between the two variables was evaluated using the Chi-square (x^2) test given in Eq. 5[21], while the coefficient of variation (CV %) was determined using Eq. 6[22].

$$Chi^2/df = x^2/n-p(\%) = 100/n-p*\sum(r_{i,exp}-r_{i,cal})^2/r_{cal} \dots\dots\dots.5$$
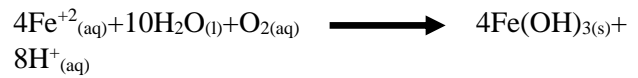
$$CV\% = [SD/mean] * 100 \dots\dots.6$$

Where, $r_{i,exp}$ and $r_{i,cal}$ represent the experimental and model-fitting values of the removal efficiency, respectively, while $\acute{r}_{i,exp}$ is the mean value of $r_{i,exp}$, n is the number of responses, p is the number of model factors, and df is the degree of freedom related to the model. For quality assurance and model applicability, the degree of fitting at the highest $r_{i,adj}$ and the lowest value of Chi^2/df represent the standard values. Table 5 show the evaluated regression coefficients, corresponding F-value, and significance level. The model would be statistically significant if the R^2 exceeded 0.8[15].

EC Process

The EC process began once the current from the external power supply was switched on. The oxidation began at the anodes, while reduction took place at cathodes. The dissolution at the anode produced Fe^{+2} ions, while OH^- ions were generated at the cathode. Mixing the released ions (Fe^{2+} and OH^-) with wastewaters gave rise to various monomeric and polymeric ions in hydrolyzed forms, depending on the concentration of Fe^{2+} ions and the pH value. These monomeric and polymeric species would adsorb pollutants to construct bigger flocs and finally settle down. These settled flocs are called sludge[23]. The formation of metal hydroxides at the pH value of 7 is given by two chemical mechanisms at the electrodes[24, 25]. The first mechanism forms $Fe(OH)_3$ precipitate at the anode while releasing hydrogen gas at the cathode. The reactions are as below:

Mechanism #1 at anode:

$$4Fe_{(s)} \longrightarrow 4Fe^{2+}_{(aq)} + 8e^-$$

$$4Fe^{+2}_{(aq)}+10H_2O_{(l)}+O_{2(aq)} \longrightarrow 4Fe(OH)_{3(s)}+8H^+_{(aq)}$$

At cathode :

$$8H^+_{(aq)} + 8e^- \longrightarrow 4H_{2(g)}$$

The overall reaction of the first mechanism is as below:

$$4Fe_{(s)}+10H_2O_{(l)}+O_{2(aq)} \longrightarrow 4Fe(OH)_{3(s)} + 4H_{2(g)}$$

In the second mechanism, $Fe(OH)_2$ precipitate is formed at the anode while hydrogen gas is released at the cathode according to the reactions shown below:

Mechanism #2 at anode:

$$Fe_{(s)} \longrightarrow Fe^{2+}_{(aq)} + 2e^-$$

$$Fe^{+2}_{(aq)}+2OH^-_{(aq)} \longrightarrow Fe(OH)_{2(s)}$$

At cathode:

$$2H_2O_{(l)}+2e^- \longrightarrow 2OH^-_{(aq)} + H_{2(g)}$$

The overall reaction of the second mechanism is as below:

$$Fe_{(s)} + 2H_2O_{(l)} \longrightarrow Fe(OH)_{2(s)} + H_{2(g)}$$

Precipitates of $Fe(OH)_{2(s)}$ and $Fe(OH)_{3(s)}$ remain in the solution as a gelatinous suspension, which can be removed from the wastewater either by complexation or by electrostatic attraction followed by coagulation. Depending on the pH values, the monomeric and polymeric species formed include $Fe(H_2O)_6^{3+}$, $Fe(H_2O)_5OH^{2+}$, $Fe(H_2O)_4(OH)^{2+}$, $Fe_2(H_2O)_8(OH)_2^{4+}$, $Fe_2(H_2O)_6(OH)_4^{2+}$, and $Fe(OH)_4^-$.

Results and Discussion

Table 1. Main characteristics of the dairy wastewater.

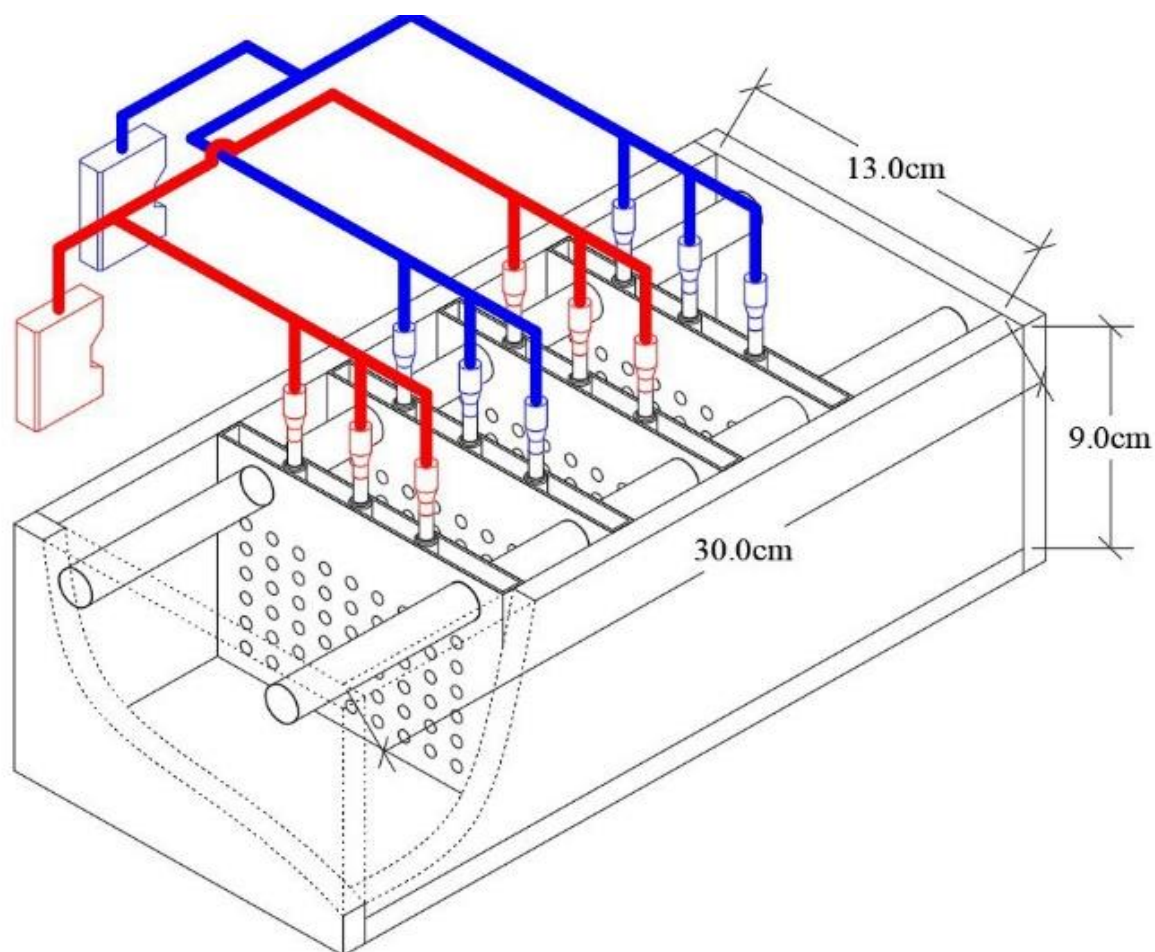| Parameter	Value
pH	6.83
BOD_5 (mg/L)	11505
COD (mg/L)	34650
Total suspended solids (mg/L)	730
Total dissolved solids (mg/L)	3667
Oil and grease	944
Nitrogen (N) (mg/L)	0.4
Phosphorous (P) (mg/L)	0.5
Iron (Fe) (mg/L)	0.3
Turbidity NTU	3080
Electrical conductivity (µs/cm)	7640

Figure 1. A schematic sketch for EC reactor and electrodes. The rods are used for supplying current overall the electrode. The connection was Monopolar design.
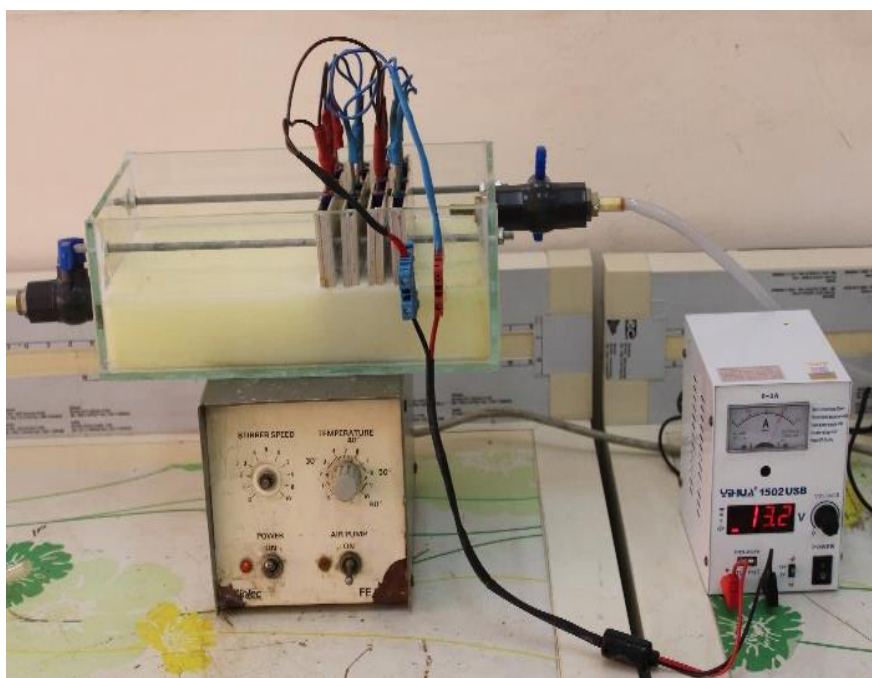
Figure 2. Main parts of the EC system (reactor and electrodes) and the current supply regulator.

Table 2. Parameters names and levels in EC process for dairy wastewater.

Parameter	Value	Reference
Distance between electrodes	(0.5, 1, 1.5, 2, 2.5 and 3 cm)	29, 35
Detention time	(10, 20, 30, 60, 90, and 120 min)	7, 40
NaCl dosage	(0, 50, 100, 250, 500, and 1000 mg/L)	48, 49
COD concentration	(C_0, $C_1/2$, $C_1/4$, $C_1/6$, $C_1/8$ and $C_1/10$ mg COD/L)	7, 40
Current Density at 15V	(2.115, 3.461, 5.384, 7.884, and 8.077 mA/cm^2)	55, 57, 58

Table 3. Ranges and coded values for the parameters.

Factors	Parameter	Units	Min. value	Max. value	Coded low	Coded high
A	Distance between electrodes	cm	0.5	2	-1	+1
B	Detention time	min	90	120	-1	+1
C	NaCl dosage	mg/L	50	350	-1	+1
D	COD concentration	mg/L	3700	4700	-1	+1
E	Current Density at 15V	mA/cm^2	3.5	8	-1	+1

Table 4. Statistical analysis of the results of EC treatment of dairy wastewater.

No.	A cm	B min	C mg/L	D mg/L	E mA/cm^2	Actual COD removal %	Predicted COD removal %
1	0.875	120	200	4700	5.57	83.1	84.2
2	2	120	50	4450	6.875	81.5	80.7
3	1.625	112.5	50	3700	3.5	72.1	70.2
4	0.875	105	350	3700	4.625	65.6	68.0
5	1.625	105	125	4700	3.5	67.8	68.5
6	0.5	105	200	4200	5.75	77.1	75.3
7	1.25	90	275	3700	6.875	74.2	71.7

8	0.5	90	125	3700	8	67.5	69.0
9	1.25	90	200	4200	3.5	75.3	72.5
10	0.5	90	50	4700	3.5	71.0	71.3
11	0.875	90	350	4700	8	62.9	65.9
12	1.625	105	125	4700	3.5	66.3	68.5
13	0.875	120	50	3950	6.875	79.6	80.9
14	2	90	50	3700	8	76.2	73.8
15	0.5	112.5	50	4450	8	82.4	81.9
16	2	120	275	3950	4.625	61.2	61.4
17	2	112.5	350	4700	8	74.2	76.3
18	2	90	50	4700	4.625	66.5	64.8
19	2	90	50	3700	3.5	70.7	74.3
20	0.5	105	200	4200	5.75	72.6	75.3
21	1.25	97.5	50	4200	5.75	70.3	71.1
22	0.5	105	200	4200	5.75	76.5	75.3
23	1.625	112.5	125	3700	8	73.9	75.4
24	2	90	125	4700	8	58.1	59.2
25	1.25	97.5	50	4200	5.75	72.8	71.1
26	0.5	120	350	3950	8	70.6	70.4
27	1.25	90	200	4200	3.5	69.6	72.5
28	2	90	350	3950	8	66.5	69.9
29	0.5	120	350	4450	3.5	77.3	77.5
30	0.5	120	50	3700	3.5	75.1	76.4
31	1.625	97.5	275	4450	6.875	70.1	68.7

Table 5. Evaluated regression coefficients, corresponding F-value, and significant level.

| Item	Value	Parameter	Relationship	F value	p-value (Prob>F)
Standard Deviation	2.42	A	Main effect linear	29.25	< 0.0001
Mean	71.94	B	Main effect linear	21.98	0.0002
C.V. %	3.37	C	Main effect linear	13.51	0.0017
R-squared (R^2)	0.9027	D	Main effect linear	2.87	0.1075
Adjusted R-squared (R^2_{adj})	0.8379	E	Main effect linear	1.55	0.2295
Predicted R-squared	0.6351	AB	Interaction Effects (cross product)	1.77	0.1997
Adeq precision	15.8169	AD	Interaction Effects (cross product)	4.07	0.0588
		AE	Interaction Effects (cross product)	15.34	0.001
		BC	Interaction Effects (cross product)	18.54	0.0004
		BD	Interaction Effects (cross product)	50.85	< 0.0001
		BE	Interaction Effects (cross product)	27.66	< 0.0001
		CD	Interaction Effects (cross product)	8.47	0.0093
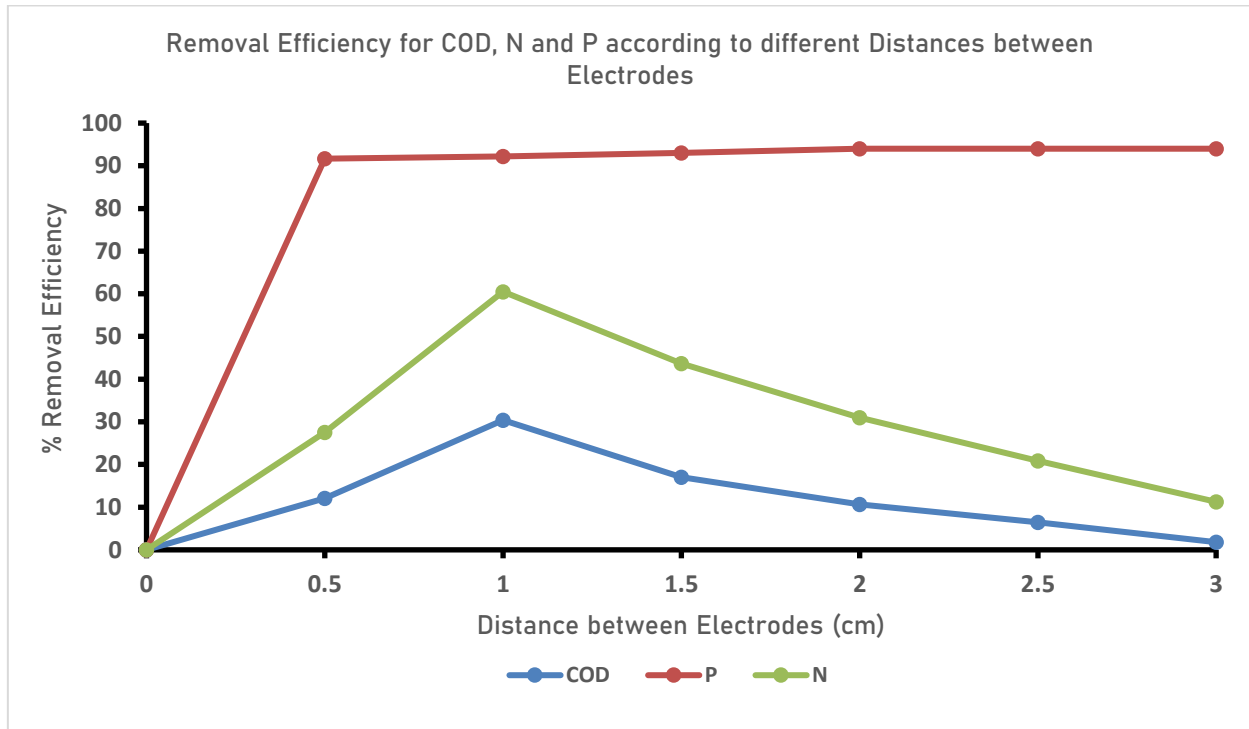
Figure 3. COD, N and P removal efficiency over different distances between electrodes. The COD concentration was 34650 mg/L, voltage 15V.
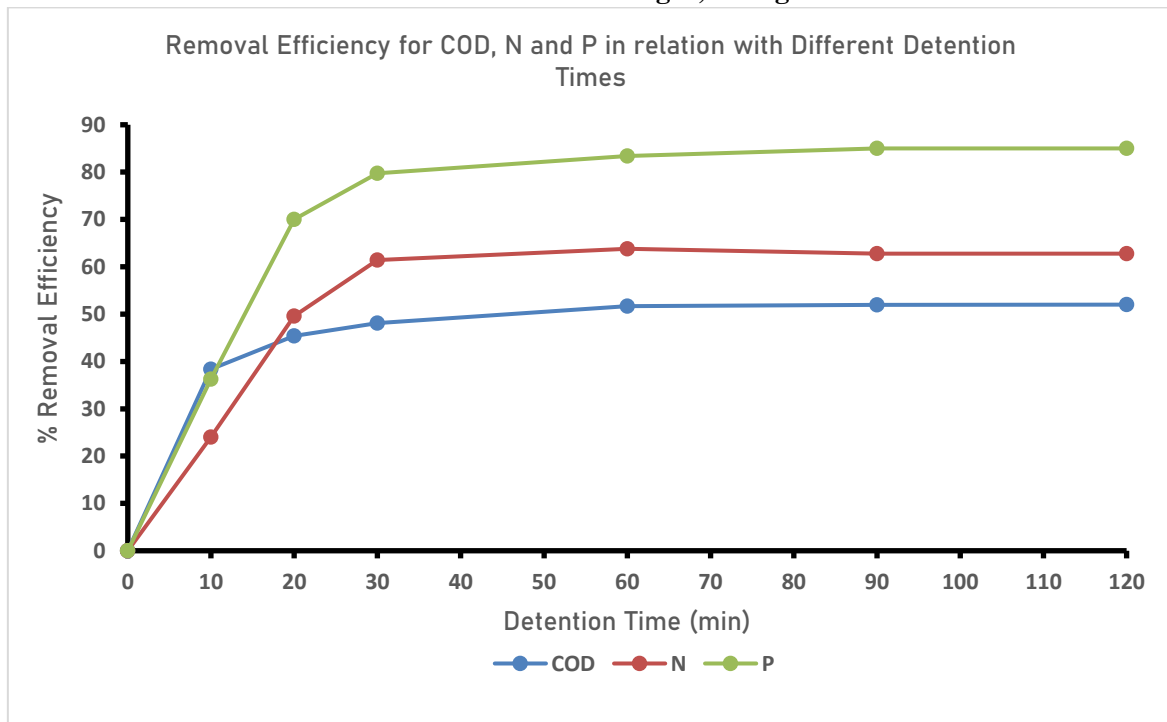

Figure 4. COD, N and P removal efficiency over different detention times, distance between electrodes 1cm, and current voltage 15V. COD concentration was 34650 mg/L.
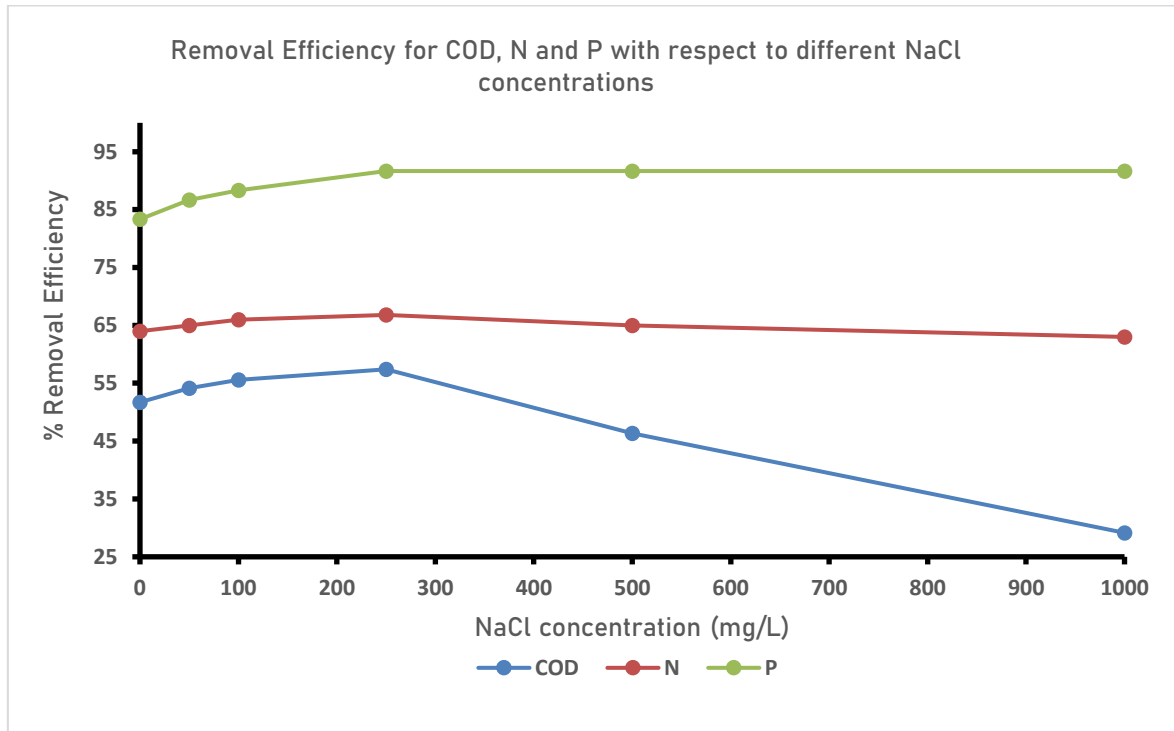
Figure 5. Removal efficiency for COD, N and P over different NaCl concentrations. Distance between electrodes equal 1cm, detention time equal 90min and current voltage 15V.
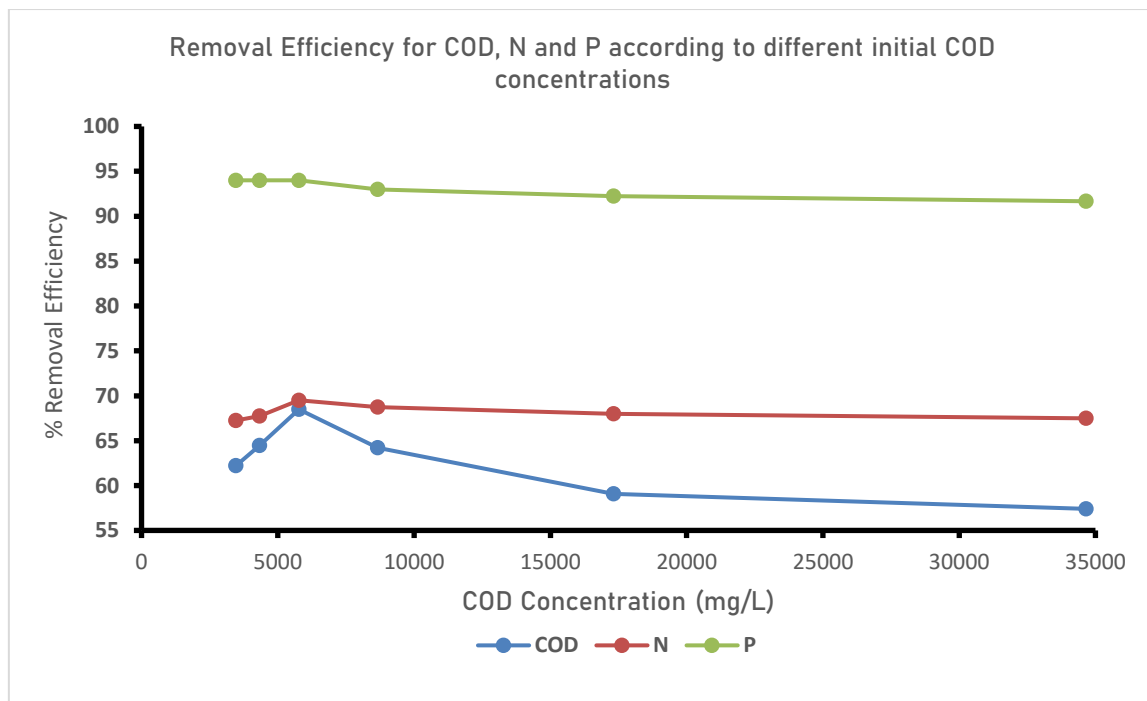

Figure 6. Removal efficiency for COD, N and P over different initial concentrations. Distance between electrodes 1cm, detention time 90min, NaCl concentration 250 mg/L and current voltage 15V.
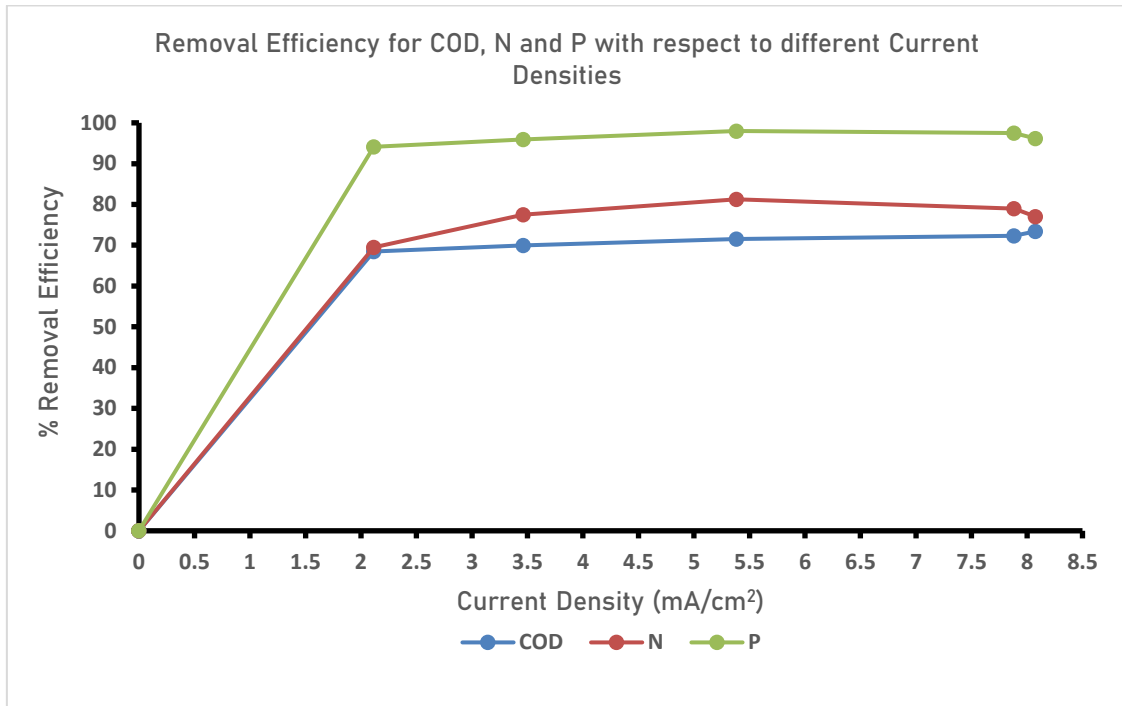
Figure 7. COD, N and P removal efficiency over different current densities. Distance between electrodes 1cm, detention time 90min, NaCl dosage 250 mg/L and COD initial concentration 5775 mg/L.
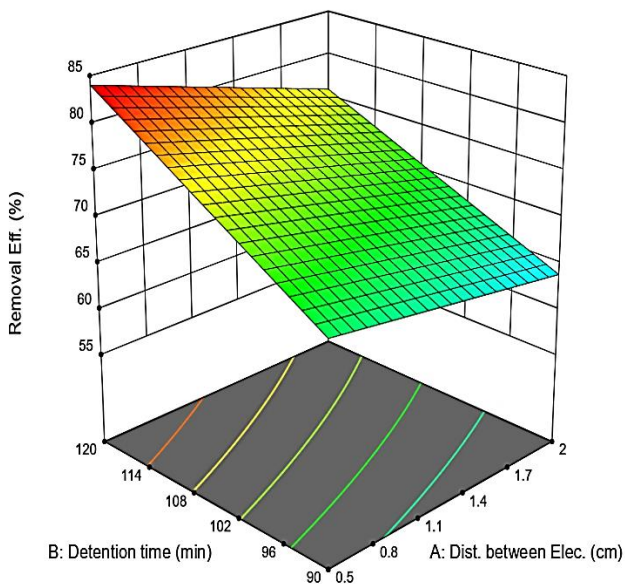

Figure 8. Effects of distance between electrodes (A) and detention time (B) over Removal efficiency for COD.
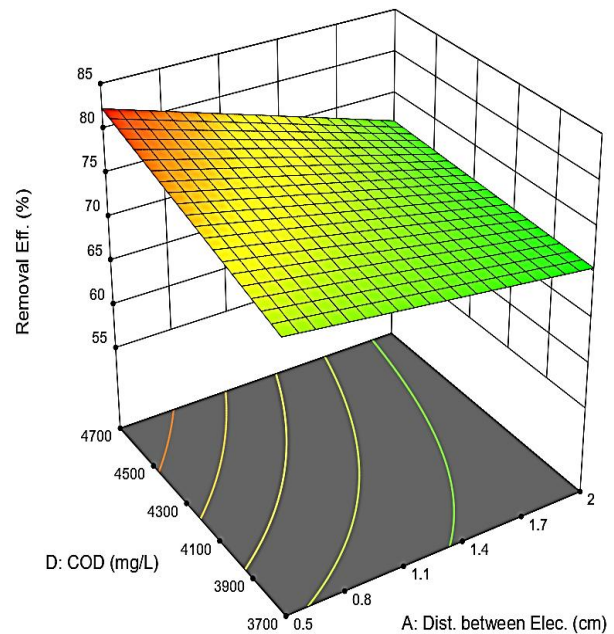

Figure 9. Effects of distance between electrodes (A) and initial concentration of COD (D) over Removal efficiency for COD.
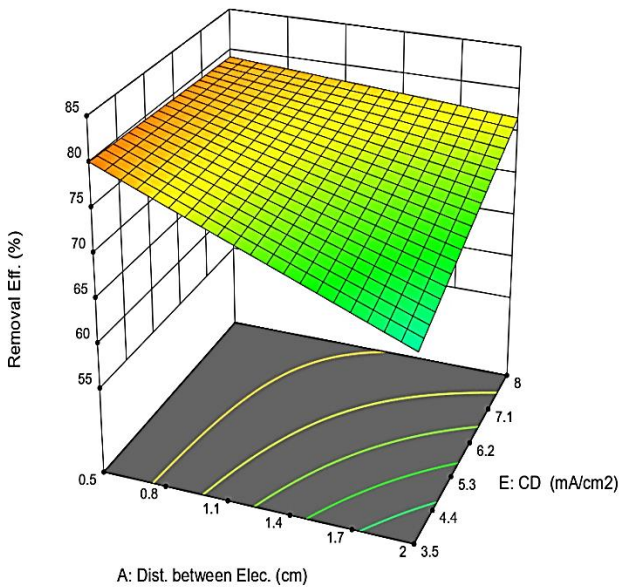
Figure 10. Effects of distance between electrodes (A) and current densities (E) over Removal efficiency for COD.
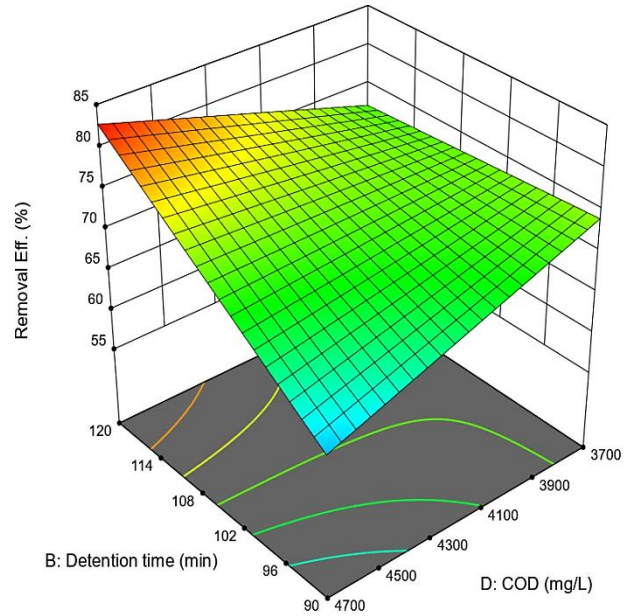

Figure 12. Effects of initial concentration of COD (D) and detention time (B) over Removal efficiency for COD.
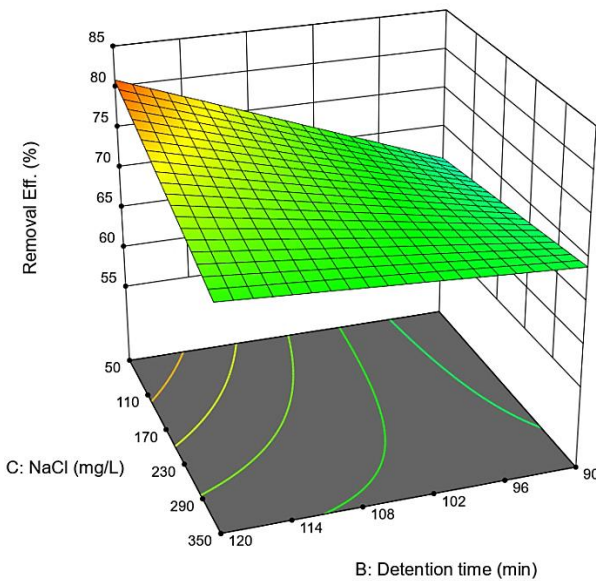

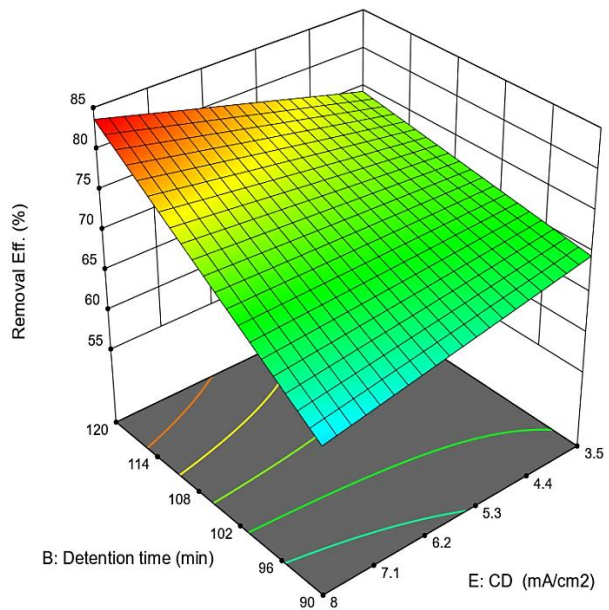**Figure 11. Effects of NaCl dosage (C) and detention time (B) over Removal efficiency for COD.**

Figure 13. Effects of detention time (B) and current density (E) over Removal efficiency for COD.
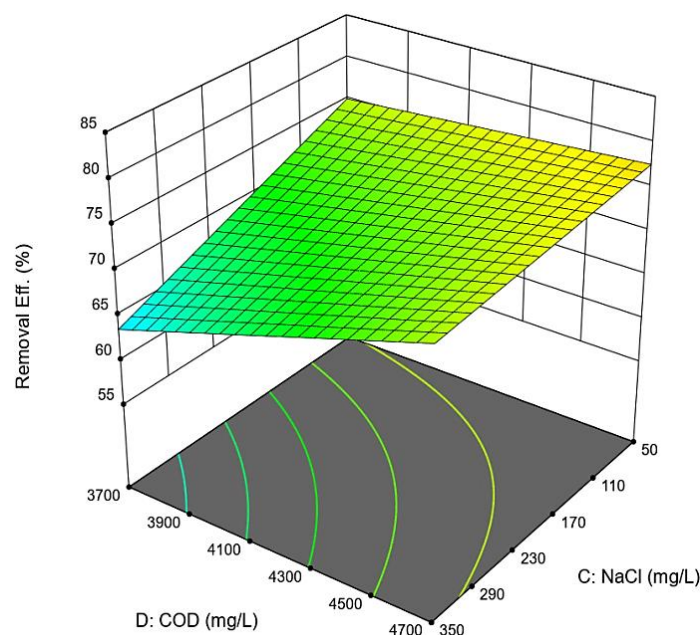
Figure 14. Effects of initial concentration of COD (D) and NaCl addition (C) over Removal efficiency for COD.

Discussion

Effects of the Parameters on Batch Experiments

Fig. 3 shows the COD removal efficiency with an optimum value of 30.4% at a distance between electrodes of 1 cm. The removal efficiency decreased as this distance increased following a reduction of the mass transfer due to the increment of Ohmic resistance. Consequently, it reduced the anodic oxidation[26, 27]. This result was consistent with the finding of a study using iron electrodes at 1 cm[20]. Likewise, a study reported that the COD removal efficiency decreased from 90.5% to 48.3% when the distance between electrodes increased from 0.8 to 2.0 cm[25]. In addition, Fig. 3. shows the optimum removal efficiency of P was 81.5%. This value was identical to the result of another study[28], suggesting that the gap between electrodes had little effect on the removal efficiency of phosphate[29]. Fig. 3 also shows the removal efficiency for N was 61.5%, and it was similar to the results of another study at 60%[30].

Figure 4 shows the optimum removal efficiency of COD which equal to 52.6% at 120 min. In general, after a significant time, EC was limited by external mass transfer on the electrodes, i.e., the Fe^{2+} and OH^- ions formed stuck on the electrode surface, growing like a film through time. Therefore, the resistance of this film reduced the EC efficiency and hence, the COD removal[31]. The removal efficiency levelled off due to an insufficient amount of flocks for the removal of pollutants. The result agrees with a study achieved optimum COD removal for dairy wastewater in 90 min at a distance of 1 cm between electrodes[32]. Fig. 4 also shows that the removal efficiency for P was proportional with time, attaining an optimum of 85% at 90 min. This result agrees with another study[33]. Meanwhile, the Figure shows an optimum removal efficiency of 64% for N was at 60 min. This result is consistent with study of optimum removal efficiency for N 67.2%[34].

Increasing the solution conductivity will elevate the removal efficiency until a specified limit and then decrease it[35]. Often, NaCl is added to increase the ionic strength of the solution[36]. On the other hand, chlorides can form different chlorine species, that enhance the oxidation reactions[37]. Fig. 5 shows that the optimum removal efficiency of COD was 57.4% at 250 mg NaCl/L. It then decreased to 29.2%, probably due to the formation of passive layers and inhibitors. These results agree with the findings of other studies[38, 39]. Fig. 5 shows that the

optimum removal efficiency of P was 91.7% at 250 mg/L. This result is consistent with the finding of another study with 92.65% removal efficiency of P[40]. Meanwhile, Fig. 5 illustrates that the removal efficiency of N was 66.7%, and this result agrees with the finding of a study with 63% removal efficiency of N[41].

The removal efficiency for pollutants usually decreases as the initial COD concentration increases at a constant current density because the amount of metal hydroxide flocs produced is insufficient to coagulate with the high number of pollutants[42]. Fig. 6 shows the optimum removal efficiency reached to 68.5%, occurred at concentration ($C_0/6$) of 5,775 mg COD/L. A study reported a 70% COD removal efficiency for dairy wastewater with an initial COD concentration of 2,000mg/L[43], while another investigation used an initial COD concentration of 4,000mg/L to treat dairy wastewater, attaining a 70% COD removal efficiency[20]. Fig. 6 shows that the optimum removal efficiency of P is equal to 94%. This result is nearly similar to the findings of other studies at 95.6%[36] and 95%[41]. By contrast, Fig. 6 shows that the optimum removal efficiency of N, reached 69.5%. Incidentally, another study attained an optimum of 71.8% removal efficiency of N when treating dairy wastewaters with Al electrodes[44].

Current density is resulted due to dividing electric current over the effective area of the anode. In general, the anodic dissolution increases along with current density[44]. However, increasing current density beyond the optimum value does not enhance removal efficiency further. Instead, it compromises the removal efficiency of pollutants due to the parasitic production of oxygen[45]. Fig. 7 shows an optimum COD removal efficiency of 73.4% at the current density of 8.077 mA/cm². A study achieved a removal efficiency of 70% for dairy wastewater at the current densities ranging from 61.7 to 308.6 A/m² [44]. Fig. 7 shows also the optimum removal efficiency of P 98% at the current density of 5.384 mA/cm². This result is consistent with other studies, including those treating synthetic dairy wastewater or using Al electrodes[46]. Meanwhile, Fig. 7 shows the optimum removal efficiency of N 81.3%. This result is nearly identical to the 81%, N removal efficiency for treating synthetic dairy wastewater with Al

electrodes[47]. In addition, a study showed treating slaughter wastewater with iron electrodes yielded an 84% N removal efficiency[48].

Model Fitting

Table 4 shows the statistical analysis of EC for the dairy wastewater, with an R^2 value of 0.9027 for the optimal design. The adjusted R^2 (0.8379) was higher than 0.8, indicating that the model was statistically significant[15]. The experimental prediction was reliable with a small coefficient of variation (CV), i.e., 3.4%[48]. The ratio of Adeq precision was 15.8, which is greater than 4, indicating that the model had a sufficiently informative signal. The adjusted R^2 and the Adeq precision ratio showed that the quadratic model was appropriate for constructing the design space and optimizing the EC process[48, 49]. Table 5 shows that the F-value of ANOVA was 13.9 with P < 0.0001, indicating that the model was statistically significant, i.e., it could navigate the design space[50]. The quadratic equation obtained is as below:

Removal%.=414.099+(12.247*A)+(-3.141*B)+(0.006*C)+(-0.074*D)+(-13.650*E)+(-0.083*A*B)+(-0.004*A*D)+(1.690*A*E)+(-0.001*B*C)+(0.0007*B*D)+(0.112*B*E)+(0.00003*C*D)

Fig. 8 shows the interaction between the distance of two electrodes (A) and detention time (B). At a higher detention time (120 min), the COD removal efficiency decreased as a result of increasing distance between electrodes. However, at a lower detention time (90 min), the COD removal efficiency decreased slightly with increasing distances between electrodes. At a higher detention time and increasing distance between electrodes, the Fe^{2+} and OH^- ions formed would stick over the electrode surface to grow like a film over time. Consequently, it yielded an extra resistance that decrease the COD removal[31]. At a lower detention time and increasing distance between electrodes, decreasing reduction in the removal efficiency was due to a reduced rate of mass transfer caused by the increment of Ohmic resistance. Together with the insufficient production of coagulants, they thus reduced the anodic oxidation[27]. At lower distance between electrodes (0.5 cm), the COD removal efficiency increased along with the detention time until the highest value,

i.e., ≈ 84%. Similarly, at a higher distance between electrodes (2 cm), the COD removal efficiency increased along with the detention time. When the distance between electrodes was shorter, more coagulants were generated, and the Ohmic resistance was minimum. At a longer distance between electrodes, the number of coagulants and the Ohmic resistance were high. The highest COD removal efficiency (84%) was attained at a distance of 0.5 cm between electrodes and a detention time of 120 min.

Fig. 9 shows the interaction between the distance of electrodes (A) and the initial COD concentration (D). At a higher initial COD concentration (4,700 mg COD/L), the removal efficiency decreased as the distance between electrodes increased. Similarly, at a lower initial concentration (3,700 mg COD/L), the removal efficiency decreased with increasing distance between electrodes. The decrease in COD removal efficiency at a higher initial concentration was due to an insufficient amount of the coagulants[42] and the increment of the Ohmic resistance when the distance between electrodes increased[27]. At a lower initial concentration, the COD removal efficiency decreased with increasing distance between electrodes at a rate lower than at a higher initial concentration, primarily due to the increment in the Ohmic resistance. When the distance between electrodes (0.5 cm) was shorter, the removal efficiency increased with increasing initial concentration. The same phenomenon happened at a longer distance between electrodes (2 cm), i.e., the COD removal efficiency increased with the increment in the initial concentration. However, the increment of removal efficiency at a shorter distance between electrodes was small between higher and lower initial concentrations, primarily due to inhibition of the passivation during the removal process. The same explanation was correct for a long distance between electrodes but with the additional high Ohmic resistance. The highest COD removal efficiency occurred at a distance of 0.5 cm between electrodes and an initial COD concentration of 4700 mg/L, or ≈ 82%.

Fig. 10 shows the reaction between the distance between electrodes (A) and current density E. When the distance between electrodes (0.5 cm) was short, the removal efficiency for COD increased slightly along with the current density until the highest value. At a longer distance between electrodes (2 cm), the removal efficiency increased drastically along with the current density. At a shorter distance, the Ohmic resistance was low, i.e., it was just sufficient to initiate the COD removal. Although the removal efficiency increased later along with the current density and anodic dissolution, the increment of current density beyond the optimum value did not enhance the removal efficiency due to the parasitic production of oxygen[45]. Also, at a higher distance between electrodes, the Ohmic resistance affected the removal efficiency. Meanwhile, at a low current density (3.5 mA/cm^2), the removal efficiency decreased drastically as the distance between electrodes increased. The same applied to high current density (8 mA/cm^2), but the removal efficiency decreased slightly with increasing distances between electrodes. At a lower current density, a fixed amount of coagulants was available. The Ohmic resistance increased along with the distance between electrodes, thus causing a drastic reduction in the removal efficiency. At a higher current density, the removal efficiency decreased slightly due to the availability of numerous coagulants. The highest removal efficiency happened at a distance of 0.5 cm between electrodes and a current density of 8 mA/cm^2, or ≈ 79%.

Fig. 11 shows the combined actions of the detention time (B) and NaCl dosage (C). At a lower dosage (50 mg NaCl/L), the COD removal efficiency increased drastically along with the detention time. Similarly, at a higher dosage (350 mg NaCl/L) the removal efficiency increased along with the detention time. Many chlorine species were formed at a higher dosage, thus affecting the removal process[51] and vice versa. Besides, at a lower detention time (90 min), the removal efficiency increased along with the NaCl dosage. At a higher detention time (120 min), the removal efficiency decreased when the NaCl dosage increased. At a lower NaCl dosage, numerous coagulants were generated but with a small amount of chlorine, thus yielding a small removal. More chlorine was formed at a high detention time when the NaCl dosage increased, hindering the removal process. The

highest removal efficiency (≈ 81%) happened at 120 min and 50 mg NaCl/L.

Fig. 12 shows the interaction between detention time (B) and the initial COD concentration (D). At a lower COD concentration (3,700 mg/L), the removal efficiency increased slightly along with the detention time. Similarly, at a high COD concentration (4,700 mg/L), the removal efficiency increased drastically along with the detention time, primarily due to ample destabilized particles coagulated with the generated monomeric and polymeric species[52]. At a lower detention time (90 min), the removal efficiency decreased when the initial concentration increased. At a higher detention time (120 min), the removal efficiency increased along with the initial concentration. The high removal efficiency was probably due to the production of more coagulants at higher detention times[53]. The optimum COD removal (≈ 84%) happened at the detention time of 120 min and the initial concentration of 4,700 mg COD/L.

Fig. 13 shows the combined action of the detention time (D) and current density E. At a lower detention time (90 min), the COD removal efficiency increased slightly along with the current density. At a higher detention time (120 min), the removal efficiency increased drastically along with the current density. Overall, the duration for generating coagulants at a higher detention time was longer than at a lower detention time. The number of coagulants generated was proportional to the time unit[54]. Meanwhile, at a lower current density (3.5 mA/cm^2),

the removal efficiency for COD increased along with the detention time. At a higher current density (8mA/cm^2), the removal efficiency increased drastically along with the detention time. More coagulants were generated at higher current density than at lower current density due to the high anodic dissociation[44], thus yielding a high COD removal efficiency. The highest COD removal efficiency (≈ 84%) happened at the detention time of 120 min and the current density of 8 mA/cm^2.

Fig. 14 shows the interaction between the NaCl dosage (C) and the initial COD concentration (D). At a lower NaCl dosage (50 mg/L), the removal efficiency increased along with the initial concentration. Also, at a higher NaCl dosage (350 mg/L), the removal efficiency increased along with the initial strength. A few chlorine species were formed at a lower NaCl dosage[51], but with high conductivity and generated more coagulants, increasing the removal. At a high dosage of NaCl, the formation of more chlorine species hindered the efficiency. By contrast, at a lower initial concentration (3,700 mg COD/L), the removal efficiency decreased slightly along with the NaCl dosage. Also, at a higher initial concentration (4,700 mg COD/L), the removal efficiency decreased marginally as the NaCl dosage increased. The removal efficiency decreased in these two cases due to passivation and the generated inhibitors[36, 38, 39]. The highest removal (≈ 77%) happened at the NaCl dosage of 50 mg/L and an initial concentration of 4,700 mg COD/L.

Conclusion

In this study, the dairy wastewater was treated using the EC technique. Electrodes were made from wasted iron materials. The five experimental variables (distance between electrodes, detention time, NaCl dosage, initial COD concentration, and current density) were optimized using the RSM-optimal design and fitted the second-order polynomial model. The analysis yielded a linear and complex interaction between parameters for predicting COD removal efficiency. The

optimum conditions for the EC treatment were: a distance of 1 cm between electrodes, a detention time of 90 min, a NaCl dosage of 250 mg/L, an initial COD concentration of 5,775 mg/L, and a current density of 8.077 mA/cm^2. The EC treatment achieved a 73.4% of COD removal efficiency, a 98.0% for phosphorous and 80.3% for nitrogen. The large surface area of the iron filings fueled the high removal efficiency.

Acknowledgment

Author's Declaration

- Conflicts of Interest: None.
- We hereby confirm that all the Figures and Tables in the manuscript are ours. Furthermore, any Figures and images, that are not mine/ours, have been included with the necessary permission for re-publication, which is attached to the manuscript.

- Ethical Clearance: The project was approved by the local ethical committee in University of Baghdad.

Author's Contribution Statement

A. W. A., M. A. A. and M. J. M. have been designed the study, "*Treatment of Dairy Wastewater by Electrocoagulation using Iron Filings Electrodes*". The total number of experiments were set by M. J. M.. All the experiments were done by A. W. A.. The analyzing and discussion for all the results were done mainly by M. A. A. and M. J. M.

The paper was written by A. W. A. under direct supervision of M. A. A. and M. J. M.

References

1. Nashaat MR Al-Bahathy IAA. Impact of Hindiya Dam on the Limnological Features ofEuphrates Riverto theNorth of Babil Governorate,Iraq. Baghdad Sci J. 2022, 19(3): 447-459. http://dx.doi.org/10.21123/bsj.2022.19.3.0447

2. Khouri L Al-Mufti MB. Assessment of surface water quality using statistical analysis methods: Orontes River (Case study). Baghdad Sci J. 2022; 19(5): 981-989. http://dx.doi.org/10.21123/bsj.2022.19.4.ID0000

3. Reilly M, Cooley AP, Tito D, Tassou SA, Theodorou MK. Electrocoagulation treatment of dairy processing and slaughterhouse wastewater. Energy procedia. 2019; 161: 343-351. http://creativecommons.org/licenses/by-nc-nd/4.0/

4. Sandoval MA, Salazar R. Electrochemical treatment of slaughterhouse and dairy wastewater: Toward making a sustainable process. Sci Dir. 2021; 26: 100662. https://doi.org/10.1016/j.coelec.2020.100662.

5. Stasinakis AS, Charalambous P, Vyrides I. Dairy wastewater management in EU: Produced amounts, existing legislation, applied treatment processes and future challenges. J Environ Manage. 2022; 303: 114152.

6. Das PP, Sharma M, Purkait MK. Recent progress on electrocoagulation process for wastewater treatment: A review. Sep Puri Techno. 2022; 292: 121058. https://doi.org/10.1016/j.seppur.2022.121058.

7. Kaur N. Different treatment techniques of dairy wastewater. Groundwater Sustain Develop. 2021;14: 100640. https://doi.org/10.1016/j.gsd.2021.100640.

8. Bajpai M, Katoch SS, Kadier A, Singh A. A review on electrocoagulation process for the removal of emerging contaminants: theory, fundamentals, and applications. Environ Sci Poll Res. 2022; 29: 15252–15281. https://doi.org/10.1007/s11356-021-18348-8.

9. Shahedi A, Darban AK, Taghipour F, Jamshidi-Zanjani A. A review on industrial wastewater treatment via electrocoagulation processes. Curr Opin Electrochem. 2020; 22: 154–169. https://doi.org/10.1016/j.coelec.2020.05.009.

10. Mohammed SJ, M-Ridha MJ, Abed KM, Elgharbawy AAM. Removal of levofloxacin and ciprofloxacin from aqueous solutions and an economic evaluation using the electrocoagulation process. Int J Environ Anal Chem. 2021; 0(0): 1-19. https://doi.org/10.1080/03067319.2021.1913733.

11. Titchou FE, Zazou H, Afanga H, El Gaayda J, Akbour RA, Hamdani M. Removal of Persistent Organic Pollutants (Pops) from Water and Wastewater by Adsorption and Electrocoagulation Process. Groundw Sustain Dev. 2021; 13: 100575. https://doi.org/10.1016/j.gsd.2021.100575.

12. Omwene PI, Celen M¸ Öncel MS, Kobya M. Arsenic removal from naturally arsenic contaminated ground

water by packed-bed electrocoagulator using Al and Fe scrap anodes. Process Saf Environ Prot. 2019; 121: 20–31. https://doi.org/10.1016/j.psep.2018.10.003.

13. Omwene PI, Celen M, Öncel MS, Kobya M. Arsenic removal from naturally arsenic contaminated ground water by packed-bed electrocoagulator using Aland Fe scrap anodes. Process Saf Environ. 2019; 121: 20–31, http://dx.doi.org/10.1016/j.psep.2018.10.003.

14. Bani-Melhem K, Al-Kilani RM, Tawalbeh M. Evaluation of scrap metallic waste electrode materials for the application in electrocoagulation treatment of wastewater. Chemosphere. 2023; 310: 136668. https://doi.org/10.1016/j.chemosphere.2022.136668.

15. M-Ridha MJ, Hussein SI, Alismaeel ZT, Atiya MA, Aziz GM. Biodegradation of reactive dyes by some bacteria using response surface methodology as an optimization technique. Alexandria Eng J. 2020; 59: 3551–3563. https://doi.org/10.1016/j.aej.2020.06.001.

16. Ya'acob A, Zainol N, Aziz NH. Application of response surface methodology for COD and ammonia removal from municipal wastewater treatment plant using acclimatized mixed culture. Heliyon. 2022; 8 (6): e09685. https://doi.org/10.1016/j.heliyon.2022.e09685.

17. Sadoon ZA and M-Ridha MJ. Optimization of the electro coagulation process for the removal of cadmium from aqueous solution using RSM. Assoc Arab Univ J Eng Sci. 2019; 26(4): 52–64. https://doi.org/10.33261/jaaru.2019.26.4.007.

18. AlJaberi FY. Modelling current efficiency and ohmic potential drop in an innovated electrocoagulation reactor. Desalin Water Treat. 2019; 164: 102-110. https://doi.org/10.5004/dwt.2019.24452.

19. Sadoon ZA M-Ridha MJ. Removal of reactive dyes by electro coagulation process from aqueous solution. J Eng. 2020: 26(2): 14-28. https://doi.org/10.31026/j.eng.2020.02.02.

20. Mohammed SJ Mohammed-Ridha MJ. Optimization of Levofloxacin removal from aqueous solution using electrocoagulation process by response surface methodology. Iraqi J Agric Sci. 2021; 52: 204.

21. Manhooei L, Mehdinejadiani B, Amininasab SM. Efficient and fast removal of nitrate from water using a novel lignocellulosic anion exchanger modified with a silane group. Desalin Water Treat. 2019; 137: 279. https://doi.org/10.5004/dwt.2019.23215.

22. Mehdinejadiani B, Amininasab SM, Manhooei L. Enhanced adsorption of nitrate from water by modified wheat straw: equilibrium, kinetic and thermodynamic studies. Water Sci Technol. 2019; 79: 302. https://doi.org/10.2166/wst.2019.047.

23. Magnisali E, Yan Q, Vayenas DV. Electrocoagulation as a revived wastewater treatment method-practical approches: a review. J Chem Technol Biotecknol. 2022; 97: 9-25. https://doi.org/10.1002/jctb.6880.

24. Visigalli S, Barberis MG, Turolla A, Canziani R, Zrimec MB, Reinhardt R, Ficara E. Electrocoagulation–flotation (ECF) for microalgae harvesting – A review. Sep Purifi Techno. 2021; 271: 118684. https://doi.org/10.1016/j.seppur.2021.118684

25. Mousazadeh M, Alizadeh SM, Frontistis Z, Kabdaslı I, Niaragh EK, Qodah Z, Naghdali Z, Mahmoud AE, Sandoval MA, Butler E, Emamjomeh MM. Electrocoagulation as a Promising Defluoridation Technology from Water: A Review of State of the Art of Removal Mechanisms and Performance Trends. Water. 2021; 13: 656. https://doi.org/10.3390/w13050656.

26. Gautam P, Kumar S. Reduction of chemical oxygen demand through electrocoagulation: an exclusive study for hazardous waste landfill leachate. Environ Sci Pollut. 2022; 29: 7583–7594. https://doi.org/10.1007/s11356-021-16214-1.

27. Oden MK. Treatment of CNC industry wastewater by electrocoagulation technology: an application through response surface methodology. Int J Env Analytical Chem. 2019; 100(1): 1-19. http://10.1080/03067319.2019.1628955.

28. Zhang X, Lin H, Hu B. A pilot-scale study of electrocoagulation on phosphorus removal from animal manure and the economic analysis. Biosys Eng. 2022; 219: 205-217. https://doi.org/10.1016/j.biosystemseng.2022.05.005.

29. Li X, Zhao X, Zhou X, Yang B. Phosphate recovery from aqueous solution via struvite crystallization based on electrochemical-decomposition of nature magnesite. J Clean Pro. 2021; 292: 126039. https://doi.org/10.1016/j.jclepro.2021.126039.

30. Atashzaban Z, Seidmohammadi A, Nematollahi D, Azarian G, Shayesteh OH, Rahmani AR. The efficiency of electrocoagulation and electroflotation processes for removal of polyvinyl acetate from synthetic effluent. Avicenna J Environ. Health Eng. 2016; 3(2): 7469. https://doi.org/10.5812/AJEHE.7469.

31. Nyangi MJ, Chebude Y, Kilulya KF, Minu A. Efects of coexisting ions on simultaneous removal of fuoride and arsenic from water by hybrid Al–Fe electrocoagulation. Inter J Environ Sci Techno. 2021. https://doi.org/10.1007/s13762-021-03598-3.

32. Nguyen QH, Watari T, Yamaguchi T, Takimoto Y, Niihara1 K, Wiff JP, Nakayama1 T. COD Removal from Artificial Wastewater by Electrocoagulation Using Aluminum Electrodes. Int J Electrochem Sci. 2020; 15: 39 – 51, https://doi.org/10.20964/2020.01.42.

33. Al-saned AJO, Kitafa BA, Badday AS. Microbial fuel cells (MFC) in the treatment of dairy wastewater. Mater Sci Eng. 2021; 1067: https://doi.org/10.1088/1757-899X/1067/1/012073.

34. Ghosh D, Medhi CR, Purkait MK. Treatment of fluoride containing drinking water by electrocoagulation using monopolar and bipolar electrode connections. Chemosphere. 2008; 73: 1393–1400.
https://doi.org/10.1016/j.chemosphere.2008.08.041.

35. Elazzouzi M, Haboubi K, Elyoubi MS. Enhancement of electrocoagulation-flotation process for urban wastewater treatment using Al and Fe electrodes: techno-economic study. Sci Dir. 2019; 13: 549-555. https://doi.org/10.1016/j.matpr.2019.04.012.

36. Kobya M, Omwene PI, Sarabia SM, Yildirima S, Ukundimana Z. Phosphorous removal from anaerobically digested municipal sludge centrate by an electrocoagulation reactor using metal (Al, Fe and Al-Fe) scrap anodes. Process Saf Environ Prot. 2021; 152: 188–200. https://doi.org/10.1016/j.psep.2021.06.003.

37. Orssatto F, Tavares MHF, Silva FM, Eyng E, Fleck L. Optimization of nitrogen and phosphorus removal from pig slaughterhouse and packing plant wastewater through electrocoagulation in a batch reactor. Ambiente e Água. 2018; 13(5): 1–10. http://dx.doi.org/10.4136/ambi-agua.2233.

38. Chezeau B, Boudriche L, Vial C, Boudjemaa A. Treatment of dairy wastewater by electrocoagulation process: Advantages of combined iron/aluminum electrodes. Sep Sci Techno. 2019; https://doi.org/10.1080/01496395.2019.1638935.

39. Sahu O, Mazumdar B, Chaudhari PK. Treatment of wastewater by electrocoagulation: a review. Environ Sci Pollut Res. 2014; 21: 2397–2413. https://doi.org/10.2166/wpt.2021.108.

40. Khandegar V, Saroha AK. Electrochemical treatment of effluent from small-scale dyeing unit. Indian Chem Eng. 2013; 55: 112–120. https://doi.org/10.1080/00194506.2013.798889.

41. Aoudj S, Khelifa A, Drouiche N. Removal of fluoride, SDS, ammonia and turbidityfrom semiconductor wastewater by combined electrocoagulation–electroflotation. Chemospher. 2017; 180: 379–387. https://doi.org/10.1016/j.chemosphere.2017.04.045.

42. Hasson D, Lumelsky V, Greenberg G, Pinhas Y, Semiat R. Development of the electrochemical scale removal technique for desalination applications. Desalination. 2008; 230: 329–342. https://doi.org/10.1016/j.desal.2008.01.004.

43. Omwenea PI, Kobyaa M, Canb OT. Phosphorus removal from domestic wastewater in electrocoagulation reactor using aluminium and iron plate hybrid anodes. Eco Eng. 2018; 123: 56-73. https://doi.org/10.1016/j.ecoleng.2018.08.025.

44. Thapa A, Rahman S, Borhan MDS. Remediation of Feedlot Nutrients Runoff by Electrocoagulation Process. Am J Environ Sci. 2015; 11(5): 366-379. https://doi.org/10.3844/ajessp.2015.366.379.

45. Dalvand A, Gholami M, Joneidi A, Mahmoodi NM. Dye removal, energy consumption and operating cost of electrocoagulation of textile wastewater as a clean process. Clean–Soil, Air, Water. 2011; 39: 665–672. https://doi.org/10.1002/clen.201000233.

46. Wang Y, Kuntke P, Saakes M, van der Weijden RD, Buisman CJN, Lei Y. Electrochemically mediated precipitation of phosphate minerals for phosphorus removal and recovery: Progress and perspective. Water Res. 2022; 209: 117891. https://doi.org/10.1016/j.watres.2021.117891.

47. Kushwaha JP, Srivastava CV, Mall ID. Organics Removal from Dairy Wastewater by Electrochemical Treatment and Residue Disposal. Sep Purif Technol. 2010; 76(2): 198-205. doi:10.1016/j.seppur.2010.10.008. https://doi.org/10.1016/j.seppur.2010.10.008.

48. Lakshmi PM, Sivashanmugam P. Treatment of oil tanning effluent by lectrocoagulation: Influence of ultrasound and hybrid electrode on COD removal. Sep Purif Technol. 2013; 116: 378–384. https://doi.org/10.1016/j.seppur.2013.05.026.

49. Bayat O, Kilic O, Bayat B, Anil M, Akarsu H, Poole C. Electrokinetic dewatering of Turkish glass sand plant tailings. Water Res. 2006; 40: 61–6. https://doi.org/10.1016/j.watres.2005.10.021.

50. Bassala HD, Dedzo GK, Bememba CBN, Seumo PMT, Dazie JD, Njiki CN, Ngameni E. Investigation of the efficiency of a designed electrocoagulation reactor: Application for dairy effluent treatment. Process Saf Environ Prot. 2017; 111: 122– 127. https://doi.org/10.1016/j.psep.2017.07.002.

51. Hiwarkar AD, Singh S, Srivastava CV, Mall ID. Mineralization of pyrrole, a recalcitrant heterocyclic compound, by electrochemical method: Multi-response optimization and degradation mechanism. J Environ Manage. 2017; 198: 144–152. https://doi.org/10.1016/j.jenvman.2017.04.051.

52. Das A, Mishra S. Removal of textile dye reactive green-19 using bacterial consortium: process optimization using responsesurface methodology and kinetics study. J Environ Chem Eng. 2017; 5: 612–627. https://doi.org/10.1016/j.jece.2016.10.005.

53. Dil EA, Ghaedi M, Ghaedi AM, Asfaram A, Goudarzi A, Hajati S, Soylak M, Agarwal S, Gupta VK. Modeling of quaternary dyes adsorption onto ZnO–NR–AC artificial neural network: analysis by derivative spectrophotometry. J Ind Eng Chem. 2016;

34: 186–197.
https://doi.org/10.1016/j.jiec.2015.11.010.

54. Díaz V, Ibá˜nez R, Gómez P, Urtiaga AM, Ortiz I. Kinetics of electrooxidation of ammonia-N, nitrites and COD from a recirculating aquaculture saline water

system using BDD anodes. Water Res. 2011; 1: 125-134 https://doi.org/10.1016/j.watres.2010.08.020.

معالجة المخلفات السائلة لمعامل الالبان بواسطة التخثير الكهربائي وباستخدام اقطاباً مصنعة من برادة الحديد

علي وهاب أحمد[1]، محمد عبد عطية السراج[2] و مهند جاسم محمد رضا[1]

[1]قسم هندسة البيئة, كلية الهندسة, جامعة بغداد، بغداد، العراق.
[2]قسم هندسة الكيمياء الحيوية, كلية الخوارزمي, جامعة بغداد، بغداد، العراق.

الخلاصة

شهدت صناعة الالبان نموا مطردا في السنوات الاخيرة، حيث تزايدت كميات الانتاج تماشياً مع الزيادات السكانية على المستوى العالمي. كما وشهدت هذه الصناعة نمواً نوعيا تمثل في زيادة عدد الانواع المنتجة من مشتقات الحليب، مما تطلب تقنيات اكثر تعقيدا في معالجة المخلفات الناتجة عن هذه الصناعات. يهدف البحث الى معالجة المخلفات السائلة لمعامل الالبان بواسطة تقنية التخثير الكهربائي الرائدة في هذا المجال وعن طريق اعادة استخدام برادة الحديد المتخلفة من صناعات الحديد واللحام كمادة اساسية في صناعة الاقطاب الكهربائية الخاصة بعملية التخثير الكهربائي. تعمل هذه المخلفات وخاصة في حالة اطلاقها مباشرة الى المياه السطحية على التأثير وتقليل تراكيز الاوكسجين المذاب وزيادة الثورات الطحلبية, مما يؤثر تاثيرا مباشرا على نشاط وتواجد الاحياء الاخرى. وبهدف تعيين الظروف الامثل لعملية التخثير, تم استخدام البرنامج الاحصائي (Response Surface Methodology) لاختبار خمسة متغيرات وبواقع ستة مستويات لكل متغير, حيث تم دراسة التأثيرات الأحادية والمركبة للمتغيرات على المتطلب الكيميائي للأوكسجين (COD). اظهرت النتائج بأن الظروف الامثل للمتغيرات كانت على النحو التالي, المسافة بين الاقطاب (1 سم), زمن التخثر (60-120 دقيقة), كمية الـ NaCl المضافة (250 ملغم/لتر), تركيز الاحمال العضوية الداخلة مقاسة كـ COD (5775 ملغم/لتر) واخيرا كثافة التيار الكهربائي المستخدم (7.884-8.077 ملي امبير/ سم2). ادى استخدام الظروف الامثل في عمل المنظومة الخاصة بالتخثير الكهربائي الى ازالة المخلفات السائلة العضوية الخاصة بمعامل الالبان مقاسة كـ COD بكفاءة بلغت 73.4%, في حين بلغت كفاءة المنظومة في ازالة الفسفور والنايتروجين المتوافرين في مخلفات معامل الالبان بصورة مطردة الى 98% للفسفور و80.3 للنايتروجين. اثبتت التجارب العملية امكانية التقنية المستخدمة في معالجة المخلفات السائلة لمعامل الالبان بجدوى اقتصادية عالية وخاصة مع استخدام برادة الحديد المتخلفة من صناعات الحديد مع ضمان التاثيرات الصديقة للبيئة.

الكلمات المفتاحية: المتطلب الكيميائي للأوكسجين، المخلفات السائلة لمعامل الالبان، التخثير الكيميائي، كفاءة الازالة.